Journal of Magnetism and Magnetic Materials 506 (2020) 166689

Contents lists available at ScienceDirect

Journal of Magnetism and Magnetic Materials

journal homepage: www.elsevier.com/locate/jmmm

Research articles

The submicron garnet film with perpendicular magnetic anisotropy prepared by liquid phase epitaxy method

Yujuan Wu[a], Qinghui Yang[a,*], Ding Zhang[a], Yuanjing Zhang[a], Yiheng Rao[a], Qiye Wen[a], Ihor I. Syvorotka[b], Huaiwu Zhang[a,*]

[a] State Key Laboratory of Electronic Thin Films and Integrated Devices, University of Electronic Science and Technology of China, Chengdu 610054, PR China
[b] Department of Crystal Physics and Technology, Scientific Research Company "Electron-Carat", Stryjska St., 202, Lviv 79031, Ukraine

ARTICLE INFO

Keywords:
Liquid phase epitaxy
Garnet films
Perpendicular magnetic anisotropy
FMR linewidth

ABSTRACT

Rare-earth iron garnet thin films with perpendicular magnetic anisotropy (PMA) have recently attracted a great deal of attention for spintronic applications. In this study, magnetic anisotropy of epitaxial garnet films was analyzed theoretically, and $(YBiLuCa)_3(FeGe)_5O_{12}$ mono-crystalline films with PMA have been successfully grown with liquid phase epitaxial (LPE) method on $Gd_3Ga_5O_{12}$ (GGG) substrates. Microstructural properties, chemical composition and magnetic properties of the epitaxial films were discussed in detail. We found that growth temperatures played a significant role in the uniaxial anisotropy of the epitaxial $(YBiLuCa)_3(FeGe)_5O_{12}$ mono-crystalline films. Ferromagnetic resonance linewidth of $(YBiLuCa)_3(FeGe)_5O_{12}$ films with thickness of 170 nm was 8.06 Oe@12 GHz, which indicated that the epitaxial $(YBiLuCa)_3(FeGe)_5O_{12}$ mono-crystalline films had a great potential application in spintronic devices.

1. Introduction

With the development of electronic information technology, the size of electronic devices has been greatly minimized, which makes the quantum effects on devices more and more significant. In 2010, Japanese scientist Y. Kajiwara and others successfully achieved the long-distance transmission of spin current by using yttrium iron garnet (YIG), which opened the door of magnetic insulating materials in the field of spintronics and made spintronics devices become a research hotspot [1]. Low damping constant of YIG thin films makes it possible to meet the requirements of low loss, high transmission speed and high-density storage of electronic devices in the future, therefore, it has attracted extensive attention from researchers [2–4]. In order to effectively manipulate and drive spin waves in garnet films, thin films should be used. Moreover, the critical value of the driving current needed to drive the magnetization reversal for out-of-plane magnetized film is much smaller than that of in-plane magnetized film, which is very essential to realize the smaller and more energy-saving spintronic devices [5,6]. Therefore, it is very important to prepare ultra-thin garnet films with perpendicular magnetic anisotropy (PMA).

Liquid phase epitaxy (LPE) method is one of the best techniques for preparing mono-crystalline garnet films. Garnet films with growth anisotropy can be induced during LPE process [7,8]. In YIG films grown by LPE, the easy-to-magnetize axis is generally parallel to the film surface. However, in doped YIG, Bi^{3+} and some rare earth ions can induce large growth-induced anisotropy, which makes it possible to prepare doped YIG films with easy magnetization axis perpendicular to the film surface by LPE [7–10]. Although mono-crystalline garnet films prepared by LPE method have very high crystal quality, it is difficult to prepare ultra-thin garnet films by LPE method because of its fast growth rates. Therefore, the preparation of ultra-thin garnet films with out-of-plane anisotropy by LPE method is a difficult problem in the field spintronics. In this study, based on these requirements, we designed a low growth rate melt formulation to prepare mono-crystalline garnet film with out-of-plane anisotropy by LPE method, and mono-crystalline garnet films with composition of $(YBiLuCa)_3(FeGe)_5O_{12}$ and ultra-thin thickness of submicron have been successfully prepared. The effect of growth conditions on specific composition, magnetic anisotropy and ferromagnetic resonance linewidth of the films were studied in detail.

2. Theoretical analysis

The magnetic anisotropy of garnet films prepared by LPE method includes cubic magnetocrystalline anisotropy, shape anisotropy and uniaxial anisotropy. These parameters are shown in Eq. (1). The uniaxial anisotropy mainly comes from lattice mismatch and growth

* Corresponding authors.
E-mail addresses: yangqinghui@uestc.edu.cn (Q. Yang), hwzhang@uestc.edu.cn (H. Zhang).

https://doi.org/10.1016/j.jmmm.2020.166689
Received 2 December 2019; Received in revised form 27 February 2020; Accepted 28 February 2020
Available online 28 February 2020
0304-8853/

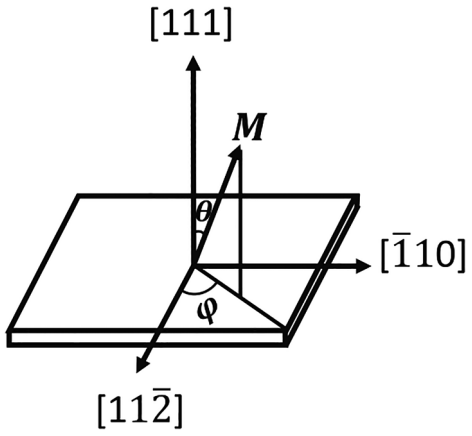

Fig. 1. Schematic diagram of total spontaneous magnetization ***M*** orientation in (1 1 1) films.

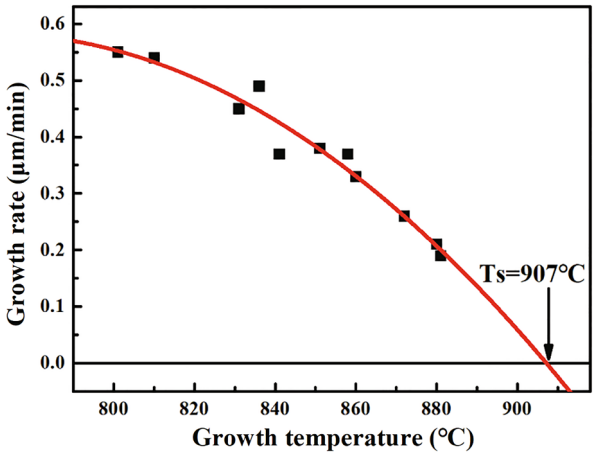

Fig. 2. Growth rate of $(YBiLuCa)_3(FeGe)_5O_{12}$ films.

conditions [8,11]. The first cubic magnetocrystalline anisotropy coefficient K_1 of (1 1 1) – oriented garnet films is negative ($\sim 10^{-4}$ deg/cm^3), which makes (1 1 1) orientation easy to be magnetized [12,13]. Therefore, gadolinium gallium garnet (GGG) substrate with (1 1 1) orientation was chosen as the substrate in our experiment. For a fixed composition, the cubic magnetocrystalline anisotropy coefficient of the film is a constant [14]. In the coordinate system shown in Fig. 1, based on the principle of minimum energy, the energy density formula of (1 1 1) crystal-oriented garnet films prepared by LPE method can be expressed by the Eq. (2) [11,14]. When θ approaches zero, the film presents PMA. In order to get the minimum of Eq. (2), θ and φ at equilibrium must satisfy: $\frac{\partial E_{total}}{\partial \theta} = 0$, $\frac{\partial E_{total}}{\partial \varphi} = 0$ and $\frac{\partial^2 E_{total}}{\partial \theta^2} \geq 0$. $\frac{\partial E_{total}}{\partial \varphi} = 0$ always holds when $\varphi = 0$, which means that Ms always lies in the $(11\bar{2})$ plane. $\frac{\partial E_{total}}{\partial \theta} = 0$ and $\frac{\partial^2 E_{total}}{\partial \theta^2} \geq 0$ are given by Eqs. (3) and (4).

$$E_{total} = E_{cubic} + E_{shape} + E_{uniaxial} \quad (1)$$

$$E_{total} = K_u sin^2\theta + 2\pi M_S^2 cos^2\theta + K_1\left(\frac{1}{4}sin^4\theta + \frac{1}{3}cos^4\theta + \frac{\sqrt{2}}{3}sin^3\theta cos\theta cos3\varphi\right) \quad (2)$$

$$\frac{\partial E_{total}}{\partial \theta} = (K_u - 2\pi M_S^2)\sin 2\theta + K_1\left\{-\frac{7}{24}sin4\theta - \frac{1}{12}sin2\theta + \frac{\sqrt{2}}{3}(3sin^2\theta - 4sin^4\theta)\right\} = 0 \quad (3)$$

$$\frac{\partial^2 E_{total}}{\partial \theta^2} = 2(K_u - 2\pi M_S^2)cos2\theta + K_1\left\{-\frac{7}{6}cos4\theta - \frac{1}{6}cos2\theta + \frac{\sqrt{2}}{3}(6sin\theta cos\theta - 16sin^3\theta cos\theta)\right\} \geq 0 \quad (4)$$

When θ approaches zero, the films obtain PMA, and we can get the result from the Eqs. (3) and (4):

$$2(K_u - 2\pi M_S^2) - \frac{4}{3}K_1 \geq 0 \quad (5)$$

where uniaxial anisotropy coefficient K_u is composed of stress-induced part K_u^{λ} and growth-induced part K_u^{g} [8,15]:

$$K_u = K_u^{\lambda} + K_u^{g} \quad (6)$$

Assuming that the garnet is an isotropic (1 1 1) film, the stress-induced K_u^{λ} is given by [16]:

$$K_u^{\lambda} = -\frac{3}{2}\frac{E}{1-\nu}\left[\frac{\Delta a}{a}\right]\lambda_{111} \quad (7)$$

where E is Young's modulus (E $\sim 2.0 \times 10^{12} dyne/cm^2$), ν is Poisson's ration ($\nu \sim 0.29$), λ_{111} is magnetostriction constant (for this film, λ_{111} is about -2.76×10^{-6}.) and $\Delta a/a$ is the ratio of $\Delta a = a_{substrate}$-a_{film} to $a = a_{substrate}$. When $\lambda_{111} < 0$ and $\Delta a > 0$, the film is under tensile stress, the easy magnetic axis prefer to be vertical to the plane of the films [14,17].

The growth-induced anisotropy K_u^{g} has not been explained satisfactorily. $K_u^{g} > 0$, the growth-induced uniaxial anisotropy perpendicular to the film surface. For the Bi-substituted garnet films, K_u^{g} increased with the Bi concentration and it is primarily controlled by the supercooling of the melt [8,15], the K_u^{g} increases linearly with the supercooling.

In summary, in order to fabricate an ultra-thin mono-crystalline film with PMA with LPE method, we need to adjust the parameters of K_1, K_u^{g} andK_u^{λ} to overcome the shape anisotropy. For (1 1 1)-oriented garnet films, $K_1 < 0$, which is beneficial for PMA. It is necessary to make K_u positive and as large as possible. As a result, the film needs to be in the state of tensile stress to get a larger growth anisotropy.

3. Experimental

Based on the above analysis, the film should be in tensile stress state and have a larger growth anisotropy. However, tensile stress state and larger growth anisotropy are contradictory. Because higher Bi content will make the lattice expand, which is harmful to the tensile stress of film. Therefore, it is necessary to select small radius ions to replace the dodecahedral position in order to balance this change.

We chose GGG (1 1 1) as the substrate, and the lattice constant of GGG is 12.383 Å, while the lattice constant of YIG is 12.376 Å. For the garnet crystal, its dodecahedron can be substituted with a variety of ions [18]. Bi^{3+} with large ionic radius can both expand the lattice constant and induce large growth-induced anisotropy, which contributes to turn the easy magnetic axis perpendicular to the film surface [7,8]. To neutralize the lattice expansion caused by the doping of Bi^{3+},

Table 1
Detailed growth parameters of $(YBiLuCa)_3(FeGe)_5O_{12}$ films.

Number	Thickness (μm)	Growth temperature(°C)	Growth rate (μm/min)	Rotation rate(r/min)	Interval of rotation reversion(s)	Growth time(min)
1	1.07	880	0.21	60	5	5
2	1.11	858	0.37	60	5	3
3	0.99	835	0.45	60	5	2
4	1.09	810	0.54	60	5	2
5	1.1	801	0.55	60	5	2

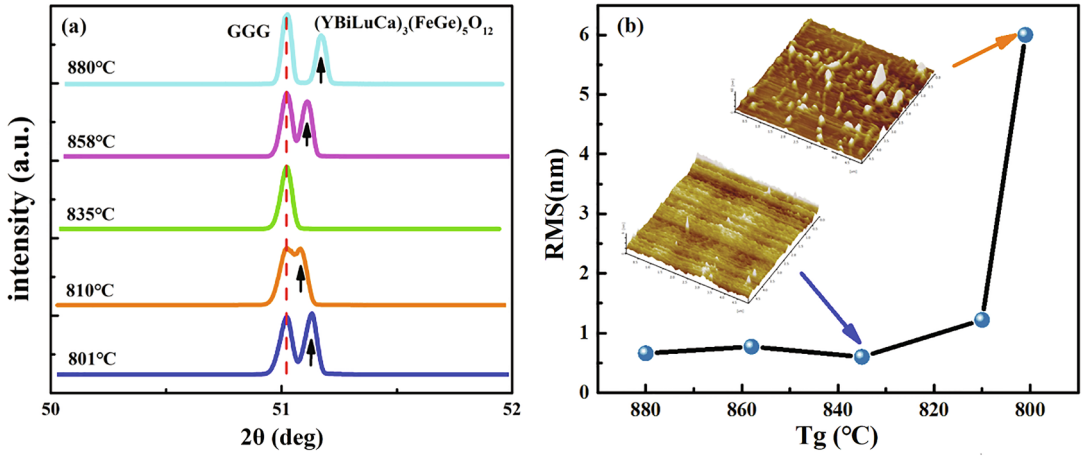

Fig.3. The XRD spectra and AFM images of $(YBiLuCa)_3(FeGe)_5O_{12}$ films, (a) XRD spectra of the films; (b) RMS values and AFM images of the films.

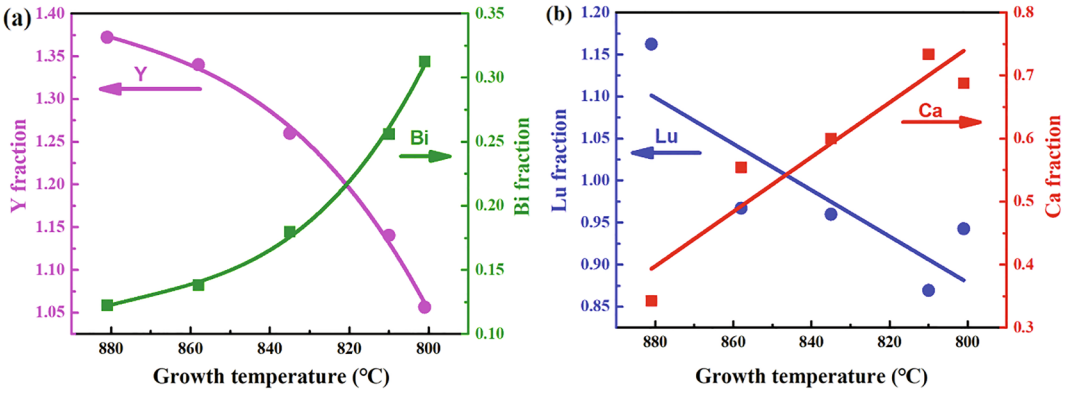

Fig. 4. Chemical concentration of Y^{3+}, Bi^{3+}, Lu^{3+}, Ca^{2+} in $(YBiLuCa)_3(FeGe)_5O_{12}$ films.

we doped Lu^{3+} with a small ionic radius. Furthermore, we chose non-magnetic ion Ge^{4+} with strong position selectivity to substitute the tetrahedral sites, which could dilute the Fe^{3+} in the crystal so as to effectively reduce the saturation magnetization of the films [19]. And this can also decrease the shape anisotropy. In order to maintain the balance of chemical, an equal amount of Ca^{2+} must be doped, and Ca^{2+} with large ion radius will occupy the dodecahedron sites. Finally, we got the $(YBiLuCa)_3(FeGe)_5O_{12}$ garnet films in the PbO-Bi_2O_3-MoO_3 flux system. The detailed growth procedures were described in our previous studies [20–22].

A series of $(YBiLuCa)_3(FeGe)_5O_{12}$ films at different growth temperature were prepared, the growth rate as a function of temperature was shown in Fig. 2. The range of the growth temperature is 800–881 ℃, which is much wider than other garnet films. The growth rate is from 0.19 to 0.55 μm/min, which present a gentle slope with temperature comparing other melts [18,23]. These facts ensure that we can prepare thin garnet films by LPE method, the smallest thickness of the films grown was 100 nm.

We chose a series of $(YBiLuCa)_3(FeGe)_5O_{12}$ films grown at different growth temperatures with a similar thickness of about 1 μm, and the detailed growth parameters are listed in Table.1. The morphological and structural properties of the $(YBiLuCa)_3(FeGe)_5O_{12}$ films were analyzed by using atomic force microscopy (AFM, SEIKO SPA-300HV, Japan) and high-resolution x-ray diffraction (HRXRD, D1 Evolution, JVS, Germany). FMR properties were measured by VNA-FMR system at room temperature, magnetic properties were analyzed through vibration sample magnetometer (VSM, BHV525, IWATSH, Japan). Chemical composition was measured by Time-of-flight secondary ion mass spectrometry instrument (TOF. SIMS 5-100, ION-TOF GmbH, Münster, Germany).

4. Results and discussion

The XRD spectra of the films grown at different temperatures was shown in Fig. 3(a), with the decreasing of the growth temperature, the mismatch first became smaller and then turned to bigger. The mismatch is as small as 0.05% at 835 ℃. The mismatch between films and substrates has a directly influence on the stress-induced anisotropy, and chemical concentration changes the lattice parameter of the films. The lattice parameter of garnet films decreased nonlinearly with the concentration of Ca^{2+} and Ge^{4+} ions, and other lattice changes of substitution for Y are listed as follows: Lu = −0.031 Å/per atom, Bi = +0.0828 Å/per atom [14]. Although the lattice parameter of $(YBiLuCa)_3(FeGe)_5O_{12}$ films increased with the growth temperature, it was always smaller than that of the GGG substrates (12.383 Å), which is conducive to the out-of-plane anisotropy. Fig. 3(b) shows the surfaces roughness RMS changing with the growth temperature. The values of RMS are small, but as the growth temperature dropped to 801 ℃, the roughness of the surfaces had a sharp increase and the films showed island structure.

Time-of-flight secondary ion mass spectrometry (ToF-SIMS) depth profiling was used to obtain the depth-dependence ration $c(R^{3+})/c(Bi^{3+})$ (R is Y, Lu, Ca, respectively.) in the prepared $(YBiLuCa)_3(FeGe)_5O_{12}$ films. In ions-substituted yttrium iron garnet structure, Y^{3+}, Bi^{3+}, Lu^{3+} and Ca^{2+} ions occupy 24 (c) position together. Therefore, it is known that the sum of the concentrations of Y^{3+}, Bi^{3+}, Lu^{3+} and Ca^{2+} is basically constant in the stoichiometric $(YBiLuCa)_3(FeGe)_5O_{12}$ films. Combining with the quantitative element analysis method of ToF-SIMS [24–26], we can calculate the relative atomic concentration in $(YBiLuCa)_3(FeGe)_5O_{12}$ films.

Fig. 4 shows the relative atomic concentration in

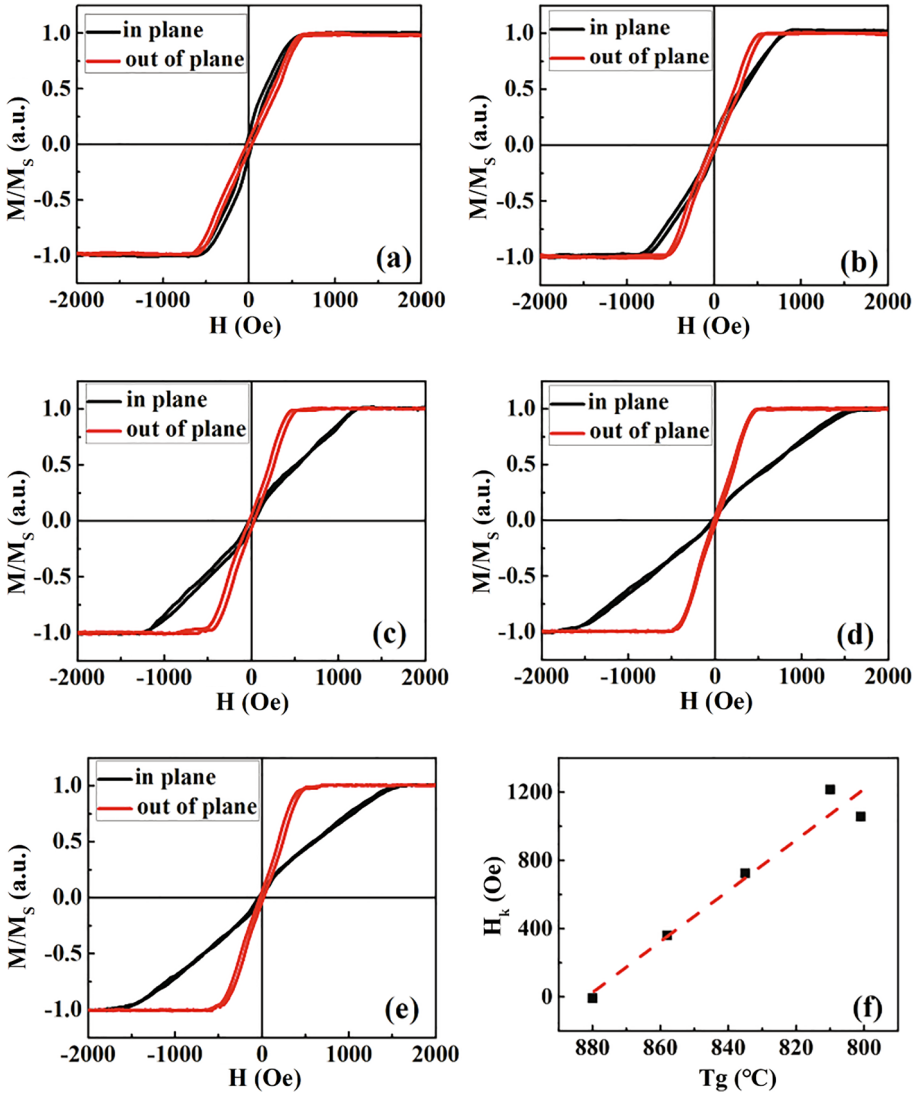

Fig. 5. (a–e) Magnetic hysteresis loops of $(YBiLuCa)_3(FeGe)_5O_{12}$ garnet films growth at different temperatures, (f) H_k changes as a function of growth temperature.

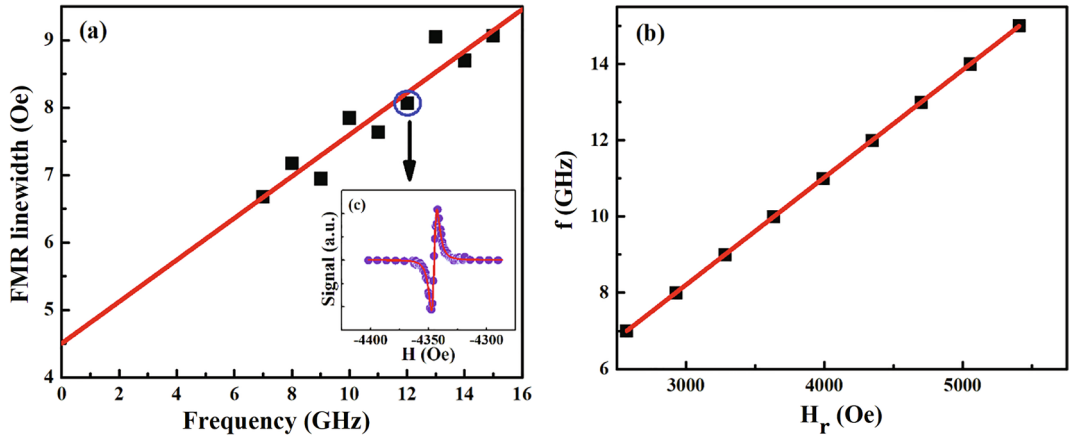

Fig. 6. FMR properties of 170-nm-thick $(YBiLuCa)_3(FeGe)_5O_{12}$ garnet film grown at 859 ℃, where the points showing experimental data and the red curves showing fits, the applied field is parallel to the film surface. (a) FMR field vs frequency; (b) FMR linewidth vs frequency; (c) FMR profile at 12 GHz.

$(YBiLuCa)_3(FeGe)_5O_{12}$ films with different growth temperatures. As growth temperature dropping, the concentration of Bi^{3+}, Ca^{2+} and Ge^{4+} increased and the concentration of Y^{3+} and Lu^{3+} decreased correspondingly. The increasing of supercooling and Bi^{3+} concentration is beneficial to increase the growth-induced anisotropy, which is beneficial to turn the magnetic easy axis to be out-of-plane.

Magnetic hysteresis loops of the $(YBiLuCa)_3(FeGe)_5O_{12}$ films grown at 880 ℃ and 810 ℃ were shown in Fig. 5(b) and (c). The results

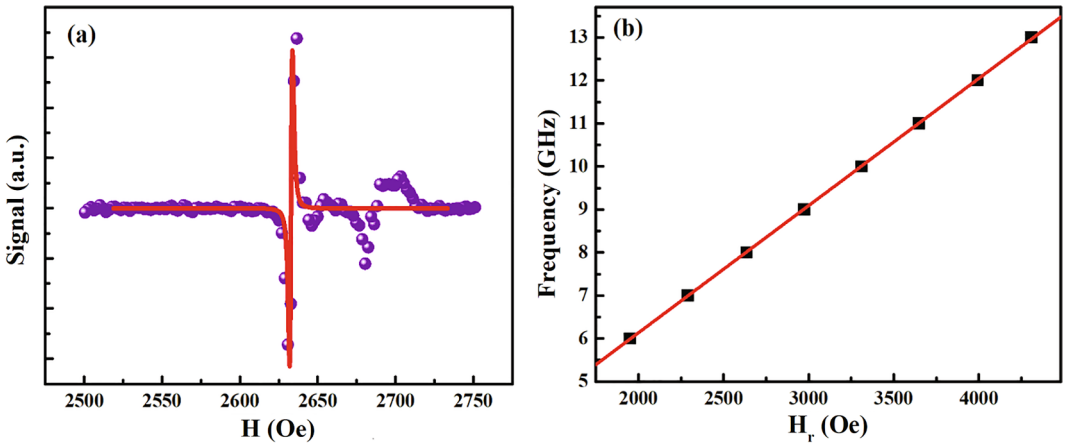

Fig. 7. FMR properties of 170-nm-thick $(YBiLuCa)_3(FeGe)_5O_{12}$ garnet film grown at 859 ℃, where the points showing experimental data and the red curves showing fits, the applied field is vertical to the film surface. (a) FMR profile at 8 GHz; (b) FMR field vs frequency.

indicated the saturation magnetization ($4\pi M_S$)of the films is about 750 Oe, which is much smaller than that of YIG. We assumed the field was $H_{s\text{-}o}$ as the films were magnetized by out-of-plane filed to saturation, and $H_{s\text{-}i}$ as the films were magnetized by in-plane filed to saturation. Fig. 5(a) shows the difference between $H_{s\text{-}i}$ and $H_{s\text{-}o}$, $H_k = H_{s\text{-}i} - H_{s\text{-}o}$, as a function of the growth temperature. The perpendicular anisotropy of the films was increased with the decreasing of the growth temperature, which was agreed with our analysis. We found that the out-of-plane orientation anisotropy of the films became very weak with the increase of growth temperature, although the films were still in a large tensile stress state, which means that growth-induced anisotropy played a dominant role in the growth of $(YBiLuCa)_3(FeGe)_5O_{12}$ films

The ferromagnetic resonance (FMR) properties were extracted from FMR measurements. The FMR spectrum was measured in a coplanar waveguide, the applied magnetic fields can be parallel or perpendicular to the film surface. The FMR linewidth ΔH as a function of microwave frequency was fitted using Eq. (8), and the resonance field was fitted using the Kittle equation, Eq. (9), where $4\pi M_{eff}$ is the effective saturation magnetization.

$$\Delta H(f) = \Delta H_0 + (2\alpha/\gamma)/2\pi f \tag{8}$$

$$f = \frac{\gamma}{2\pi}\sqrt{H_r(H_r + 4\pi M_{eff})} \tag{9}$$

Fig. 6 presents FMR properties of $(YBiLuCa)_3(FeGe)_5O_{12}$ film with thickness of 170 nm (in-plane field). The frequency of the microwaves was ranging from 7 GHz to 15 GHz. As shown in this figure, gyromagnetic ratio $|\gamma|$ is 2.94 MHz/Oe, FMR linewidth ΔH is 8.06 Oe@ 12 GHz and the damping constant α is 4.33×10^{-4} of these films. The gyromagnetic ratio $|\gamma|$ and damping constant α are slightly higher than that of pure YIG (~2.8, $\sim 10^{-5}$) [27]. In Fig. 7, the results of the corresponding out-of-plane field configuration are given. In Fig. 7(a), additional resonance peaks appear at the FMR shoulder because of the additional spin-wave resonance modes are activated. According to the fitting, gyromagnetic ratio $|\gamma|$ of the film is 2.96 MHz/Oe, which is approximately equal to that tested under in-plane field. These facts clearly demonstrated that the epitaxial $(YBiLuCa)_3(FeGe)_5O_{12}$ films prepared in this paper are suitable for spintronics.

5. Conclusion

In conclusion, $(YBiLuCa)_3(FeGe)_5O_{12}$ mono-crystalline garnet films with PMA were prepared with LPE method in this study. Cubic magnetocrystalline anisotropy, growth-induced anisotropy and stress-induced anisotropy are the key factors during preparing mono-crystalline garnet films with PMA. The out-of-plane magnetic anisotropy of the epitaxial $(YBiLuCa)_3(FeGe)_5O_{12}$ mono-crystalling films increases with the decreases of growth temperatures. The growth-induced anisotropy controlled by supercooling play a significant role in manipulating magnetic anisotropy of LPE growth films. The small damping constant ($\alpha = 4.33 \times 10^{-4}$) makes the epitaxial films have a broad application prospect in spintronics.

CRediT authorship contribution statement

Yujuan Wu: Formal analysis, Investigation, Data curation, Writing - original draft. **Qinghui Yang:** Conceptualization, Methodology, Writing - review & editing, Supervision. **Ding Zhang:** Writing - review & editing. **Yuanjing Zhang:** Data curation, Writing - original draft, Visualization. **Yiheng Rao:** Writing - review & editing. **Qiye Wen:** Writing - review & editing. **Ihor I. Syvorotka:** Writing - review & editing. **Huaiwu Zhang:** Writing - review & editing, Supervision.

Declaration of Competing Interest

The authors declare that they have no known competing financial interests or personal relationships that could have appeared to influence the work reported in this paper.

Acknowledgements

This work was supported by the International Cooperation Project under Grant No. SQ2018YFE020560, National Key Research and Development Plan under Grant No. 2016YFA0300801, National Natural Science Foundation of China under Grant Nos. 51472046, 51272036, 51002021, 61131005, 61831012 and 51572042, National Key Scientific Instrument and Equipment Development Project under Grant No. 51827802 and Science Challenge Project under Grant No. TZ2018003.

References

[1] Y. Kajiwara, K. Harii, S. Takahashi, et al., Transmission of electrical signals by spin-wave interconversion in a magnetic insulator, Nature 464 (7286) (2010) 262–266, https://doi.org/10.1038/nature08876.
[2] A. Krysztofik, H. Głowiński, P. Kuświk, et al., Characterization of spin wave propagation in (111) YIG thin films with large anisotropy, J. Phys. D Appl. Phys. 50 (23) (2017) 235004, , https://doi.org/10.1088/1361-6463/aa6df0.
[3] M. Evelt, V.E. Demidov, V. Bessonov, et al., High-efficiency control of spin-wave propagation in ultra-thin yttrium iron garnet by the spin-orbit torque, Appl. Phys. Lett. 108 (17) (2016) 172406, , https://doi.org/10.1063/1.4948252.
[4] T. Chiba, G.E.W. Bauer, S. Takahashi, Current-induced spin-torque resonance of magnetic insulators, Phys. Rev. B 2 (3) (2014) 034003, , https://doi.org/10.1103/PhysRevApplied.2.034003.
[5] J. Fu, M. Hua, X. Wen, et al., Epitaxial growth of $Y_3Fe_5O_{12}$ thin films with perpendicular magnetic anisotropy, Appl. Phys. Lett. 110 (20) (2017) 202403, ,

https://doi.org/10.1063/1.4983783.
[6] C.O. Avci, A. Quindeau, C.F. Pai, et al., Current-induced switching in a magnetic insulator, Nat. Mater. 16 (3) (2017) 309–314, https://doi.org/10.1038/nmat4812.
[7] P. Hansen, C.P. Klages, K. Witter, Growth-induced anisotropy and Faraday rotation of bismuth-substituted europium-iron-garnet films, J. Appl. Phys. 63 (6) (1988) 2058–2064, https://doi.org/10.1063/1.341108.
[8] P. Hansen, K. Witter, Growth-induced uniaxial anisotropy of bismuth-substituted iron-garnet films, J. Appl. Phys. 58 (1) (1985) 454–459, https://doi.org/10.1063/1.335645.
[9] A.V. Zenkov, A.S. Moskvin, Bismuth-induced increase of the magneto-optical effects in iron garnets: a theoretical analysis, J. Phys. Condens. Matter 14 (28) (2002) 6957, https://doi.org/10.1088/0253-6102/49/1/28.
[10] P. Hansen, W. Tolksdorf, K. Witter, et al., Recent advances of bismuth garnet materials research for bubble and magneto-optical applications, IEEE Trans. Magn. 20 (5) (1984) 1099–1104, https://doi.org/10.1109/TMAG.1984.1063479.
[11] H. Makino, Y. Hidaka, Determination of magnetic anisotropy constants for bubble garnet epitaxial films using field orientation dependence in ferromagnetic resonances, Mater. Res. Bull. 16 (8) (1981) 957–966, https://doi.org/10.1016/0025-5408(81)90137-9.
[12] A.H. Bobeck, E.G. Spencer, L.G. Van Uitert, et al., Uniaxial magnetic garnets for domain wall "BUBBLE" devices, Appl. Phys. Lett. 17 (3) (1970) 131–134, https://doi.org/10.1063/1.1653335.
[13] N. Adachi, T. Yamaguchi, T. Okuda, et al., In-plane magnetic anisotropy of (111) and (100) garnet film prepared for magneto-optical indicator, J. Magn. Magn. Mater. 272 (2004) 2255–2256, https://doi.org/10.1016/j.jmmm.2003.12.580.
[14] A.H. Eschenfelder, A.H. Bobeck, Magnetic bubble technology, Phys. Today 33 (1980) 55, https://doi.org/10.1063/1.2914212.
[15] P. Hansen, K. Witter, W. Tolksdorf, Magnetic and magneto-optic properties of lead- and bismuth-substituted yttrium iron garnet films, Phys. Rev. B 27 (11) (1983) 6608, https://doi.org/10.1103/PhysRevB.27.6608.
[16] B. Hoekstra, J.M. Robertson, W.T. Stacy, The origin of the uniaxial anisotropy in thin films of $(YLaPb)_3(FeGa)_5O_{12}$ and its variation along the growth direction, Mater. Res. Bull. 12 (1) (1977) 53–64, https://doi.org/10.1016/0025-5408(77)90088-5.
[17] S. Tkachuk, V.J. Fratello, C. Krafft, et al., Imaging capabilities of bismuth iron garnet films with low growth-induced uniaxial anisotropy, IEEE Trans. Magn. 45 (10) (2009) 4238–4241, https://doi.org/10.1109/TMAG.2009.2025384.
[18] Peter Capper, Michael Mauk (Eds.), Liquid Phase Epitaxy of Electronic, Optical and Optoelectronic Materials, John Wiley & Sons, 2007.
[19] G. Vertesy, Distribution of tetravalent substituting ions in magnetic sublattices in $(YSmCA)_3(FeGe)_5O_{12}$ epitaxial garnet films, J. Phys. D Appl. Phys. 21 (12) (1988) 1833, https://doi.org/10.1088/0022-3727/21/12/030.
[20] D. Zhang, Q. Yang, M. Wang, et al., Effect of substrate defects on LIDT of $(BiTm)_3(GaFe)_5O_{12}$ films grown by LPE, Appl. Surf. Sci. 484 (2019) 169–174, https://doi.org/10.1016/j.apsusc.2019.04.102.
[21] D. Zhang, Q. Yang, Y. Jiang, et al., Laser-induced damage of garnet films grown by LPE, Opt. Mater. 91 (2019) 268–273, https://doi.org/10.1016/j.optmat.2019.03.034.
[22] D. Zhang, Q. Yang, J. Hao, et al., Effect of lattice mismatch on the laser-induced damage thresholds of $(BiTm)_3(GaFe)_5O_{12}$ thin films, Appl. Surf. Sci. 473 (2019) 235–241, https://doi.org/10.1016/j.apsusc.2018.12.053.
[23] D. Zhang, B. Mei, H. Zhang, et al., Liquid-phase epitaxial growth of 3 in diameter bismuth-doped thulium iron garnet films for magneto-optical applications, IEEE Trans. Magn. 51 (11) (2015) 1–3, https://doi.org/10.1109/TMAG.2015.2439714.
[24] Y.P. Kim, M.Y. Hong, J. Kim, et al., Quantitative analysis of surface-immobilized protein by TOF-SIMS: effects of protein orientation and trehalose additive, Anal. Chem. 79 (4) (2007) 1377–1385, https://doi.org/10.1021/ac0616005.
[25] K. Kaufmann, S. Wahl, S. Meyer, et al., Quantitative elemental analysis of photovoltaic Cu (In, Ga) Se_2 thin films using MCs^+ clusters, Surf. Interface. Anal. 45 (1) (2013) 434–436, https://doi.org/10.1002/sia.4950.
[26] Z.X. Jiang, K. Kim, J. Lerma, et al., Quantitative SIMS analysis of SiGe composition with low energy O^{2+} beams, Appl. Surf. Sci. 252 (19) (2006) 7262–7264, https://doi.org/10.1016/j.apsusc.2006.02.175.
[27] T. Liu, H. Chang, V. Vlaminck, et al., Ferromagnetic resonance of sputtered yttrium iron garnet nanometer films, J. Appl. Phys. 115 (17) (2014) 17A501, https://doi.org/10.1063/1.4852135.